Isospin transport effects in nuclear reactions at 25 MeV/nucleon

I. Lombardo,[1,3,*] C. Agodi,[1] R. Alba,[1] F. Amorini,[1] A. Anzalone,[1] I. Berceanu,[9] G. Cardella,[2] S. Cavallaro,[1,3] M. B. Chatterjee,[4] E. De Filippo,[2] A. Di Pietro,[1] P. Figuera,[1] E. Geraci,[2,3] G. Giuliani,[2,3] L. Grassi,[2,3] A. Grzeszczuk,[8] J. Han,[1] E. La Guidara,[3,5] G. Lanzalone,[1,6] N. Le Neindre,[7] C. Maiolino,[1] A. Pagano,[2] M. Papa,[2] S. Pirrone,[2] G. Politi,[2,3] A. Pop,[9] F. Porto,[1,3] F. Rizzo,[1,3] P. Russotto,[1,3] D. Santonocito,[1] and G. Verde[2]

[1]*Istituto Nazionale di Fisica Nucleare-Laboratori Nazionali del Sud, Via S. Sofia, Catania, Italy*

[2]*Istituto Nazionale di Fisica Nucleare-Sezione di Catania, Via S. Sofia, I-95123 Catania, Italy*

[3]*Dipartimento di Fisica e Astronomia, Università di Catania, Via S. Sofia, Catania, Italy*

[4]*Saha Institute of Nuclear Physics, Kolkata, India*

[5]*Centro Siciliano di Fisica Nucleare e Struttura della Materia, Catania, Italy*

[6]*Università Kore di Enna, Enna, Italy*

[7]*LPC Caen, CNRS-IN_2P_3, ENSICAEN, Université de Caen, Caen, France*

[8]*Institute of Physics, University of Silesia, Katowice, Poland*

[9]*Institute for Physics and Nuclear Engineering, Bucharest, Romania*

(Received 25 March 2010; published 12 July 2010)

Isotopic effects are studied in reactions induced by ^{40}Ca projectiles at 25 MeV/nucleon on ^{40}Ca, ^{48}Ca, and ^{46}Ti targets. The N/Z contents of projectilelike and midvelocity (MV) sources are probed by means of isotopic (^{7}Li/^{6}Li and ^{9}Be/^{7}Be) and isobaric (^{7}Li/^{7}Be) yield ratios, for semiperipheral events. In particular, information about isospin transport phenomena will be discussed. Isospin diffusion processes involving nuclei, which have noticeable differences in N/Z have been investigated. Signals of isospin drift, which are related to the gradient of density in the participant region, have also been observed for fragments emitted at MV.

DOI: 10.1103/PhysRevC.82.014608 PACS number(s): 25.70.Lm, 25.70.Mn

I. INTRODUCTION

Nuclear reactions at intermediate energies (20–50 MeV/nucleon) offer a unique opportunity to explore nuclear dynamics and the equation of state of infinite nuclear matter [1–9]. An interesting physical case is constituted by nuclear collisions, where the projectile and the target nuclei have similar masses but noticeably different N/Z values. In a used picture, the interacting nuclei are seen as being constituted of a mixture of two different types of fluids (neutrons and protons), and their exchange can be studied by means of transport physics (isospin transport) [2,10,11]. Isospin transport phenomena have two different facets, commonly called isospin diffusion and isospin drift. Isospin diffusion is related to the differences in concentration of neutrons and protons in the interacting projectile and target nuclei. If the interaction time between projectile and target is long enough, as for the case of low bombarding energies ($E < 10$ MeV/nucleon), the nucleon exchange process leads to a uniform distribution of the N/Z asymmetry throughout the dinuclear system [12]. By increasing the bombarding energies, the interaction time is reduced, and the N/Z degree of freedom does not have time to distribute equally between the two main reaction partners [13,14].

The interaction time also depends on the impact parameter of the collision. Therefore, isospin may distribute nonuniformly even at lower incident energies, provided that the impact parameter is large enough. In this case, the reaction partners may interact for a short time, and their mutual exchange of particles does not lead to a uniform N/Z distribution through the whole system.

The second facet of isospin transport phenomena is represented by isospin drift. This effect is related to the gradient of nuclear density, which involves the overlap region between the interacting nuclei; in particular, dynamical calculations suggest that the strong compression-expansion mechanism, which occurs in the overlap region during the first phase of the collision may lead to a neutron migration from the spectators to the low-density neck regions, by inducing a neutron enrichment of light fragments emitted at midvelocity (MV). This effect is noticeable in the case of intermediate energy collisions; in this case, the density gradient is typically larger than 10%, and the neutron enrichment of matter, which belongs to the MV region becomes clearly visible [15,16].

Generally, when nuclei that have different N/Z values collide, isospin drift and isospin diffusion phenomena simultaneously affect the MV emission. This point makes it difficult to separate the individual contribution of these two phenomena from the neutron richness of the emitted fragments. A simple but strong probe to analyze isospin drift effects without contamination because of isospin diffusion components is obtained by colliding two nuclei, which have identical N/Z values (such as, for example, $^{40}\mathrm{Ca} + {}^{40}\mathrm{Ca}$) at intermediate energies. In this special case, the isospin diffusion phenomenon is absent, and the possible neutron enrichment of light fragments emitted at MV can be attributed purely to isospin drift effects [17]. From a theoretical point of view, isospin diffusion and drift phenomena could give

*ilombardo@lns.infn.it

 ©2010 The American Physical Society

useful information about the poorly known behavior of the density-dependent part of the isovectorial term in the nuclear equation of state [6].

Experimentally, the N/Z values of the quasiprojectile (QP), the quasitarget (QT), and the MV sources can be probed by measuring isotopic distributions of produced fragments [18–20]. One can alternatively use the ratio between the yields of isobar nuclei such as $Y(n)/Y(p)$, $Y(^3\mathrm{H})/Y(^3\mathrm{He})$, $Y(^7\mathrm{Li})/Y(^7\mathrm{Be})$, and $Y(^{11}\mathrm{B})/Y(^{11}\mathrm{C})$. These approaches are based on the assumption that these isobaric ratios reflect the initial neutron-proton composition (N/Z) of their emitting sources [19,21]. The use of these yield ratio observables allows one to infer the N/Z of primary emitting sources with reduced contamination from secondary decays [22].

In this work, we report on isospin transport phenomena by looking at the production of isotopes (^{6,7}Li and ^{7,9}Be) and isobars (^{7}Li and ^{7}Be) in $^{40}\mathrm{Ca} + {}^{40,48}\mathrm{Ca}$, ^{46}Ti collisions at 25 MeV/nucleon (Sec. II). The ratios between the yields of neutron-rich and neutron-poor isotopes (i.e., ^{7}Li/^{6}Li and ^{9}Be/^{7}Be) as a function of the longitudinal velocity are studied in Sec. III. Section IV is devoted to the emission of isobars by studying kinetic-energy spectra of ^{7}Li and ^{7}Be fragments. The results shown in Secs. III and IV seem to confirm the presence of isospin transport effects.

II. EXPERIMENTAL APPARATUS

The experiment was performed at the Istituto Nazionale di Fisica Nucleare-Laboratori Nazionali del Sud (INFN-LNS) Super Conducting Cyclotron facility in Catania (Italy). A beam of ^{40}Ca at 25 MeV/nucleon impinged on self-supporting isotopically enriched targets of ^{40}Ca (1.24 mg/cm^2), ^{48}Ca (2.87 mg/cm^2), and ^{46}Ti (1.06 mg/cm^2). Emitted fragments were detected by the Charged Heavy Ions Mass and Energy Resolving Array (CHIMERA) 4π array. It is constituted by 1192 Si-CsI(Tl) telescopes, which cover $\simeq$94% of the whole solid angle. The mean thickness of Si detectors is 300 μm, while CsI(Tl) detectors have different thicknesses as a function of the polar angle. Details about the array and its detection and identification capabilities are described in Refs. [23–26]. We only analyzed events where the total detected charge was between 80% and 100% of the total charge Z_{tot} in the entrance channels ($Z_{\mathrm{tot}} = 40$ and 42 for Ca and Ti targets, respectively). Quasielastic reactions were removed during the experiment by the chosen electronics trigger condition, which requires the detection of at least three charged particles with $Z > 1$.

This work focuses on the detection of different isotopes and isobars, as ^{6}Li, ^{7}Li, and ^{7}Be, ^{9}Be identified by means of the $\Delta E - E$ energy-loss technique in the Si-CsI(Tl) telescopes of CHIMERA. The resulting identification threshold is about 7 MeV/nucleon. The kinetic energies of identified fragments are measured from the energy deposited in the silicon detectors, with an uncertainty $\Delta E/E_{\mathrm{kin}} \approx 2\%$ for a single telescope. Silicon energy calibration was obtained by using elastic scattering of different low-energy beams, combined with calibrated pulser signals to prove the linearity of the electronics, and checked with punch through energies of various nuclear species.

III. ISOTOPIC EMISSION

Isospin effects can be investigated by measuring the ratio between the yields of a pair of isotopes as a function of their parallel velocity [27,28]. This is shown in Fig. 1 for ^{6}Li/^{7}Li and ^{7}Be/^{9}Be yield ratios. In the upper panel of Fig. 1, we show inclusive results, while the lower panel shows the results obtained for events selected with charged particle multiplicity $m_{cp} \leqslant 6$. We can consider m_{cp} roughly as an impact parameter selector, as suggested in Ref. [29]. In this case, the used gate on m_{cp} selects mostly semiperipheral collision events. Even if the absolute values of isotopic ratios are slightly smaller than the inclusive case (especially for Be isotopes), the trends are similar.

Isotopic ratios for fragments emitted with longitudinal velocities near the projectile one ($v_{\mathrm{par}} \approx 0.2c$) in different reaction systems are noticeably different. The interest in this observation relies on the fact that the beam nucleus used in all three reactions was the same (^{40}Ca) with $N/Z = 1$. Indeed, this effect seems to be directly related to the N/Z of the differently used *targets*. We observe, in the region of $v_{\mathrm{par}} \approx v_{\mathrm{par}}^{\mathrm{proj}}$, an enhancement in the emission of neutron-rich isotopes for the reaction, which involves the *target* with larger neutron excess (^{48}Ca, $N/Z = 1.4$) as compared to the other two targets (^{40}Ca and ^{46}Ti, by having, respectively, $N/Z = 1$ and $N/Z = 1.09$). This effect is probably caused by the fact that it is possible, in semiperipheral reactions, to observe isospin diffusion effects especially for the reaction, which involves projectile and target

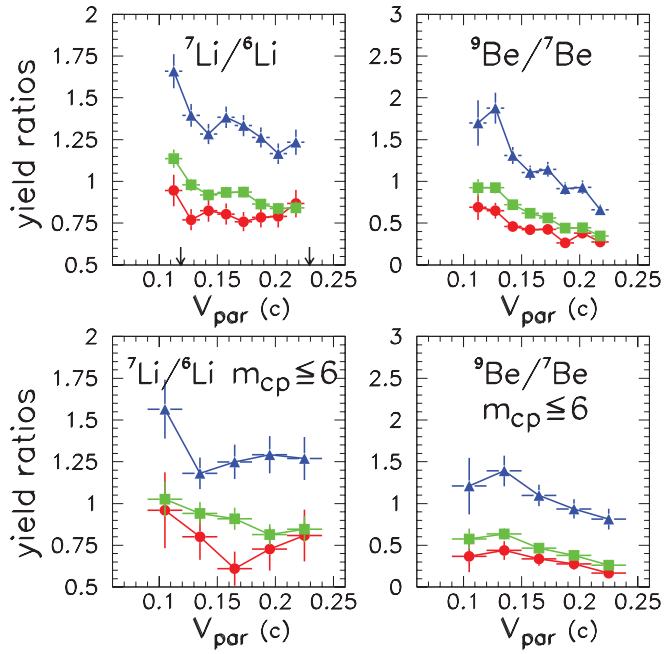

FIG. 1. (Color online) (Upper panel) ^{7}Li/^{6}Li (left) and ^{9}Be/^{7}Be (right) isotope yield ratios as a function of the longitudinal velocity in the laboratory frame without any gate on the impact parameter. (Lower panel) Same distributions obtained in semiperipheral events ($m_{cp} \leqslant 6$). Blue triangles: $^{40}\mathrm{Ca} + {}^{48}\mathrm{Ca}$ reaction. Green squares: $^{40}\mathrm{Ca} + {}^{46}$Ti reaction. Red circles: $^{40}\mathrm{Ca} + {}^{40}\mathrm{Ca}$ reaction. The arrows in the upper left panel indicate projectile velocity and half of projectile velocity.

nuclei with a larger gradient in N/Z (^{40}Ca + ^{48}Ca). This phenomenon leads to an increase of the N/Z of the QP source, which we experimentally infer by observing the increased isotopic yield ratio in the region of $v_{\rm par} \approx v_{\rm par}^{\rm proj}$.

The method of isotopic yield ratios has the advantage of being established between isotopes that experience almost the same Coulomb interaction when they are emitted by a given source. However, it has the disadvantage of involving isotopes (i.e., nuclei with different masses) that contribute differently to the excitation energy removal. For those reasons, and to have additional information about the isotopic composition of the different fragmenting sources, we also studied the yield ratios of light mirror nuclei ^{7}Li and ^{7}Be.

IV. MIRROR ISOBAR YIELD RATIOS

It has been shown that a way for extracting information on the N/Z content of a given emitting source consists of measuring the yield ratios of pairs of light isobars, such as $t/^3$He or ^{7}Li/^{7}Be [19,21]. Figure 2 shows ^{7}Li (left) and ^{7}Be (right) kinetic-energy spectra (black circles with error bars) measured at polar angles $\theta = 11.5, 14.5, 18, 22, 27, 34, 42, 50, 58, 66^\circ$ in the laboratory frame for the three studied reactions.

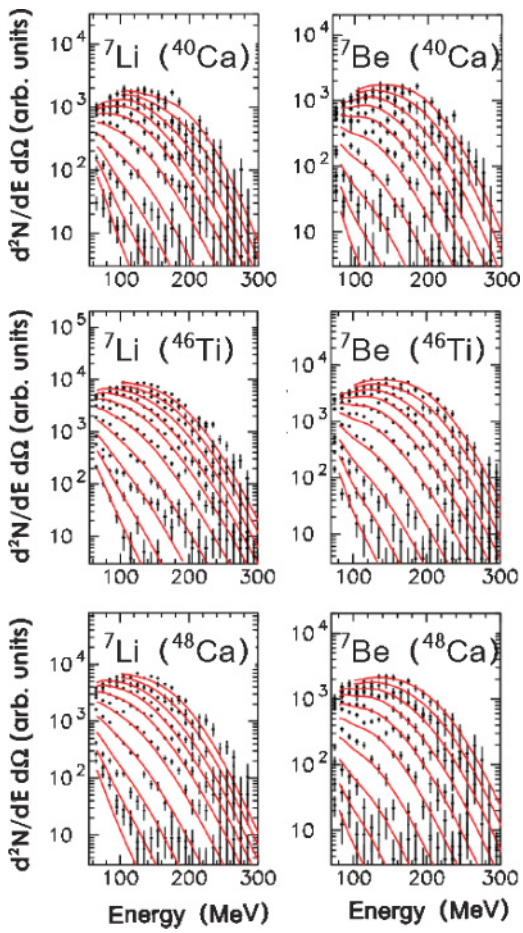

FIG. 2. (Color online) Inclusive energy spectra ($d^2N/dE\,d\Omega$) of ^{7}Li (left) and ^{7}Be (right) nuclei emitted in ^{40}Ca + ^{40,48}Ca, ^{46}Ti reactions, at different polar angles ($\theta = 11.5, 14.5, 18, 22, 27, 34, 42, 50, 58, 66^\circ$, respectively, for uppermost data points and below). The solid line represents the result of the three moving source fits, as described in the text.

To increase the statistics, we perform data analysis on inclusive events by taking into account that, for geometrical reasons, the bulk of events that belong to such a class is widely dominated by semiperipheral collisions (as already indicated in Fig. 1). We performed a multicomponent moving source analysis of these energy spectra [30–32]. In particular, we fit the energy spectra with the superposition of three Maxwellian distributions of the form [30,31,33]:

$$\frac{d^2N}{dE\,d\Omega} = \sum_{i=1}^{3} N_i \sqrt{E - E_c}\,\exp \times \left[-\frac{E - E_c + E_{S,i} - 2\sqrt{(E - E_c)E_{S,i}}\,\cos\theta}{T_i} \right]. \quad (1)$$

The ith source emits at temperature T_i and moves along the beam axis with a velocity $v_{S,i}$ in the laboratory reference frame. In Eq. (1), $E_{S,i} = \frac{1}{2} m {v_{S,i}}^2$ is the kinetic energy of a particle that moves with a velocity equal to the one of the emitting sources. The normalization constants N_i, temperatures T_i, velocities of sources $v_{S,i}$, and Coulomb barrier E_c, are determined as free parameters from the best-fit to the experimental data. Solid lines in Fig. 2 show the results of the fitting procedure. The overall agreement with the measured energy spectra is satisfactory.

We also tried to fit the spectra with only two moving sources, which represent the QP and the MV emissions (whose emitted fragments are easily detected and are identified by CHIMERA telescopes due to kinematics). The result of this two-component fit is that the spectra of particles emitted at the higher polar angles ($\theta \geqslant 50^\circ$) are not well reproduced. Experimental data can be reasonably well described only if a third source, which corresponds to QT emission is included in the fit procedure (see solid lines in Fig. 2). The contributions of the QT, MV, and QP Maxwellian moving sources are individually shown in Fig. 3, for the reaction on ^{46}Ti. The obtained fit parameters are in reasonable agreement with values reported in the literature for heavier reaction systems at slightly higher beam energy [33]. The obtained velocities of the three moving sources are $v_{S,i} = 0.06$, 0.13, and 0.19 c for QT, MV, and QP, respectively, with uncertainties of $\simeq$15%. The value obtained for the velocity associated with QT emission is slightly higher as compared to the value expected for perfect binary kinematics ($\approx 0.04c$). These effects are probably caused by identification thresholds effects affecting the reconstruction of QT emission [34]. The slope parameters ($T \approx 5$ MeV) for projectilelike and targetlike sources are comparable, by simply reflecting the overall mass symmetry in the entrance channels of the three studied reactions. For the QT source, we observe slightly larger values for the slope parameters of ^{7}Li as compared to ^{7}Be. The slope parameters obtained for the MV source are high ($T \approx 10$ MeV) in all the studied reactions. Probably this effect is caused by high dissipative friction modes, which involve the overlap region between the colliding nuclei [1,2]. In this scenario, the MV source

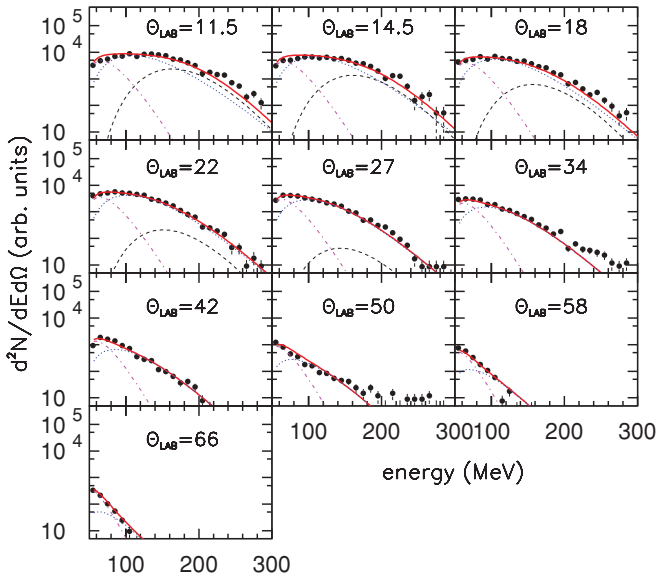

FIG. 3. (Color online) Kinetic-energy spectra of ^{7}Li nuclei emitted in the ^{40}Ca + ^{46}Ti reaction, at different values of polar angle in the laboratory frame (a similar behavior has been observed for the other two reactions). Black dashed line: QP emission. Violet dashed-dotted line: QT emission. Blue dotted line: MV emission. Red thick line: sum of the three contributions.

could be considered as an ancestor of the fireball produced at midrapidity in heavy-ion collisions at higher beam energies ($E > 70$ MeV/nucleon) [2].

^{7}Li and ^{7}Be production cross sections $\sigma_i(^{7}\mathrm{Li})$ and $\sigma_i(^{7}\mathrm{Be})$ for the ith source can be estimated by means of the expression $\sigma_i = 2N_i(\pi T_i)^{3/2}$, with N_i and T_i deduced from the best-fit analysis shown in Figs. 2 and 3 [30,31]. Then, we calculate the isobaric ratios $r_7 = \frac{\sigma_i(^{7}\mathrm{Li})}{\sigma_i(^{7}\mathrm{Be})}$ for each reaction and for QP- and MV-emitting sources. In Fig. 4, we show the obtained r_7 values for all the reactions (different symbols) and MV- and QP-emitting sources (horizontal axis).

In this figure, we observe an MV emission characterized by r_7 values higher than the QP emission ones also for the isospin symmetric reaction ^{40}Ca + ^{40}Ca. This finding is in agreement

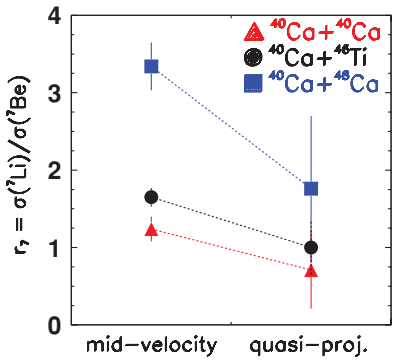

FIG. 4. (Color online) Isobaric yield ratios ^{7}Li/^{7}Be for the three different reactions ^{40}Ca + ^{40,48}Ca, ^{46}Ti at 25 MeV/nucleon, as obtained from the moving source analysis. Reconstructed QP and MV emissions are shown.

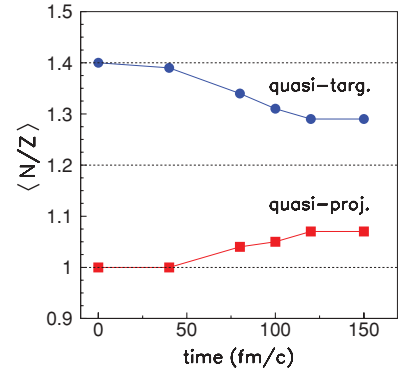

FIG. 5. (Color online) N/Z evolution of QP and QT reaction partners as seen in CoMD-II calculations for ^{40}Ca + ^{48}Ca at 25 MeV/nucleon at $b = 7$ fm. The reseparation time of the dinuclear system is $\simeq$150 fm/c. Blue circles: QT. Red squares: QP.

with the results shown in Sec. III, obtained by studying the longitudinal velocity emission of light isotopes. We confirm that, in the MV region, neutron-rich isotopes and isobars are emitted with higher probability with respect to a QP source.

By studying the isobar emission by the QP source (rightmost data points in Fig. 4), we observe that even if the projectile used was the same for the three reactions (^{40}Ca), the r_7 values increase with the N/Z of the target nucleus. This effect, in agreement with the experimental findings of Sec. III, shows that isospin diffusion takes place between projectile and target nuclei. During the collision process, the two reaction partners exchange neutrons and protons. In particular, the larger is the difference in N/Z between projectile and target nuclei, and the larger is the net neutron diffusion along the whole dinuclear system formed during the nuclear reaction.

We performed calculations of midperipheral ^{40}Ca + ^{48}Ca collisions at 25 MeV/nucleon with Constrained Molecular Dynamics (CoMD-II) [35,36], Boltzmann-Nordheim-Vlasov (BNV) [37], and Isospin Boltzmann Uehling Uhlenbeck (IBUU04) [38] codes, by looking at the N/Z evolution of QP and QT sources up to the reseparation time ($\simeq$150 fm/c). The three codes give a qualitatively similar behavior for this observable. In Fig. 5, we show, for example, the results of CoMD-II calculations at $b = 7$ fm, where we used an asy-stiff option for the symmetry potential [35]. As a result of the complex dynamics that involve the early stages of the collisions, the N/Z ratio of the two interacting partners changes as a function of time, by trying to reach a similar intermediate value. Moreover, calculations show that the complete charge equilibrium value ($N/Z = 1.2$) is not reached at the reseparation.

V. CONCLUSIONS AND PERSPECTIVES

Isospin effects involving semiperipheral nuclear reactions at 25 MeV/nucleon have been investigated by studying the emission of light isotopes (^{6,7}Li,^{7,9}Be) and isobars (^{7}Li and ^{7}Be). A neutron enrichment of nuclear clusters emitted at MV is observed by studying isobaric yield ratios. Our results are in agreement with scenarios that link these effects to isospin drift

and diffusion processes in the nuclear medium. Especially, the observed neutron enrichment at midrapidity in the case of an N/Z-symmetric reaction (^{40}Ca + ^{40}Ca) may be explained as being solely caused by the effect of isospin drifting along the low-density neck region. In the case of ^{40}Ca + ^{48}Ca N/Z-asymmetric reactions, isobaric and isotopic yield ratios show that a net diffusion of neutrons from the neutron-rich target ^{48}Ca to the ^{40}Ca projectile has occurred as a consequence of isospin diffusion effects between the interacting nuclear systems.

Isospin diffusion phenomena have been observed at higher incident energies (50 MeV/nucleon [14]) and have been used to probe the density dependence of the symmetry energy. Our work shows that such phenomena may still be important at lower incident energies. This conclusion opens interesting perspectives in view of studying isospin effects in nuclear dynamics at energies that will be available at future radioactive beam facilities. In this respect, the larger N/Z range that will be explored by these facilities will allow one to increase the sensitivity of the observed phenomena to the asymmetry potential in nuclear matter. Moreover, with the recent tuning of the pulse-shape technique for the CHIMERA silicon detectors, it will be possible to considerably lower the isotopic identification thresholds (≈3 MeV/nucleon for Li and Be isotopes [39,40]); this improvement will allow a better reconstruction of the QT emission.

ACKNOWLEDGMENTS

We thank the INFN-LNS accelerator staff for delivering beams of good quality. We thank Dr. M. Colonna for performing BNV calculations and for stimulating suggestions. We thank Dr. Bao-An Li and Dr. Lie-Wen Chen for making the IBUU04 code available to us. We also thank Professor M. Di Toro for interesting discussions about the subjects of this paper.

[1] D. A. Bromley, *Treatise on Heavy Ion Science* (Plenum, New York, 1984), Vol. 2.
[2] M. Di Toro *et al.*, Eur. Phys. J. A **30**, 65 (2006).
[3] M. Papa *et al.*, Phys. Rev. C **75**, 054616 (2007).
[4] E. De Filippo *et al.*, Phys. Rev. C **71**, 044602 (2005).
[5] E. Geraci *et al.*, Nucl. Phys. A **734**, 524 (2004).
[6] B. A. Li and W. U. Schröder, *Isospin Physics in Heavy Ion Collisions at Intermediate Energies* (Nova Science, Hauppauge, New York, 2001).
[7] F. Amorini *et al.*, Phys. Rev. Lett. **102**, 112701 (2009).
[8] I. Lombardo *et al.*, Nucl. Phys. A **834**, 458 (2010).
[9] S. Piantelli *et al.*, Phys. Rev. Lett. **88**, 052701 (2002).
[10] V. Baran *et al.*, Phys. Rep. **410**, 335 (2005).
[11] Bao-An Li *et al.*, Phys. Rep. **464**, 113 (2008).
[12] B. Gatty *et al.*, Nucl. Phys. A **253**, 511 (1975).
[13] R. Planeta *et al.*, Phys. Rev. C **38**, 195 (1988).
[14] M. B. Tsang *et al.*, Phys. Rev. Lett. **92**, 062701 (2004); M. Colonna *et al.*, Eur. Phys. J. A **30**, 165 (2006); V. Baran *et al.*, Nucl. Phys. A **730**, 329 (2004).
[15] J. Łukasik *et al.*, Phys. Rev. C **55**, 1906 (1997).
[16] J. Tõke *et al.*, Phys. Rev. Lett. **75**, 2920 (1995).
[17] R. Lionti *et al.*, Phys. Lett. B **625**, 33 (2005).
[18] E. Galichet *et al.*, Phys. Rev. C **79**, 064614 (2009).
[19] M. Veselsky *et al.*, Phys. Rev. C **62**, 041605(R) (2000).
[20] E. De Filippo *et al.*, Acta Phys. Pol. B **40**, 1199 (2009).
[21] M. B. Tsang, Y. Zhang, P. Danielewicz, M. Famiano, Z. Li, W. G. Lynch, and A. W. Steiner, Phys Rev. Lett. **102**, 122701 (2009).
[22] W. P. Tan *et al.*, Phys. Rev. C **64**, 051901(R) (2001).
[23] A. Pagano *et al.*, Nucl. Phys. A **734**, 504 (2004).
[24] F. Porto *et al.*, Acta Phys. Pol. B **31**, 1489 (2000).
[25] N. Le Neindre *et al.*, Nucl. Instrum. Methods Phys. Res. A **490**, 251 (2002).
[26] M. Alderighi *et al.*, Nucl. Instrum. Methods Phys. Res. A **489**, 257 (2002).
[27] E. De Filippo *et al.*, Acta Phys. Pol. B **37**, 199 (2006).
[28] R. Planeta *et al.*, Phys. Rev. C **77**, 014610 (2008).
[29] C. Cavata, M. Demoulins, J. Gosset, M.-C. Lemaire, D. L'Hôte, J. Poitou, and O. Valette, Phys. Rev. C **42**, 1760 (1990).
[30] T. C. Awes, S. Saini, G. Poggi, C. K. Gelbke, D. Cha, R. Legrain, and G. D. Westfall, Phys. Rev. C **25**, 2361 (1982).
[31] G. Lanzanò *et al.*, Phys. Rev. C **58**, 281 (1998).
[32] D. Santonocito *et al.*, Phys. Rev. C **66**, 044619 (2002).
[33] D. V. Shetty *et al.*, Phys. Rev. C **68**, 054605 (2003).
[34] I. Lombardo *et al.*, *CERN-Proceedings-2010-001, 12th International Conference on Nuclear Reaction Mechanisms, 15–19 June 2009, Varenna, Italy*, edited by F. Cerutti and A. Ferrari.
[35] M. Papa and G. Giuliani, Eur. Phys. J. A **39**, 117 (2009).
[36] M. Papa, T. Maruyama, and A. Bonasera, Phys. Rev. C **64**, 024612 (2001).
[37] M. Colonna, M. Di Toro, and A. Guarnera, Nucl. Phys. A **580**, 313 (1994).
[38] B. A. Li, G. C. Yong, and W. Zuo, Phys. Rev. C **71**, 014608 (2005).
[39] M. Alderighi *et al.*, Nucl. Phys. A **734**, E88 (2004).
[40] M. Alderighi *et al.*, IEEE Trans. Nucl. Sci. **52**, 1624 (2005).